

片式电容 Sn96.5/Ag3/Cu0.5 焊点热疲劳性能比较

毛书勤^{1,2}, 刘 剑¹, 葛 兵¹

(1. 长春光学精密机械与物理研究所, 长春 130031; 2. 中国科学院大学, 北京 100039)

摘 要: 以 0805 封装片式电容器焊点为研究对象, 建立了多周期温度冲击下 Sn96.5/Ag3/Cu0.5 的焊点有限元分析模型, 开展了多周期温度冲击条件下焊点剪切力测试工作, 获得了 Sn96.5/Ag3/Cu0.5 和 Sn63/Pb37 两种焊点的周期-剪切力测试数据, 并利用非线性最小二乘法得到了 1 500 个周期内的焊点热疲劳状态拟合曲线. 结果表明, 在规定试验条件下, 在有限的 1 500 个周期内 0805 封装电容的 Sn96.5/Ag3/Cu0.5 焊点的热疲劳劣化速率略慢于 Sn63/Pb37 焊点.

关键词: 片式焊点; 热疲劳状态; 剪切力

中图分类号: TG 454 文献标识码: A 文章编号: 0253-360X(2017)03-0117-04

0 序 言

铅对人体神经系统有着明显的毒害作用, 出于对环保和人类健康的考量, 欧盟 ROHS 指令中明确规定“自 2006 年 7 月 1 日起, 进入市场的电力电子产品不能含有铅、汞、镉、六价铬、聚合溴化联苯和聚合溴化联苯乙醚等六种有毒有害物质”. 信息产业部于 2007 年 3 月 1 日颁布了《电子信息产品污染控制管理办法》, 明确了对金属铅的使用限制. 无铅化已经成为电子装联行业重要的发展方向. 在无铅化推进过程中, 无铅焊点的热疲劳可靠性问题一直备受关注. 目前焊点的热疲劳问题的研究多集中在以有限元分析为基础, 对片式元件焊点、QFP 焊点、含空洞焊点、BGA 焊点等多种焊点进行建模, 结合 Manson-Coffin 方程并根据材料特性, 确定焊点在特定试验条件下的疲劳寿命. 研究多集中在焊点模型的差异性、试验条件的差异性上, 但该方法缺乏试验数据的验证. 在焊点的疲劳试验中以疲劳试验机测试和“阻值法”测试为主^[1-4]. 但是这两种方法存在测试针对性不强和阻值测量随环境温度变化的缺点.

为解决无铅焊点在实际应用过程中处于复杂应力条件下的热疲劳状态监测问题, 提出了一种基于剪切力测试的片式元件焊点热疲劳状态监测方法. 该方法具有及时性强、表征性强、受环境因素影响小的特点.

1 焊点有限元模型建立及分析

1.1 焊点有限元模型的建立

焊点的有限元模型建立与分析常用来解决两方面问题. 一个是尽可能多的考虑材料、尺寸、焊点空洞、钎料量等因素, 最大限度的逼近真实焊点, 从而获取定量数据, 代入公式后用于预测焊点的疲劳寿命; 另一个是进行合理的简化, 进行定性分析, 主要目的是获取应力、应变集中区域等信息, 进而分析疲劳、断裂等可能首先发生的部位^[5,6]. 这里进行有限元分析的主要目的是后者. 在对元器件焊点建立有限元模型之前有必要进行适当的简化和计算说明.

模型的简化. 多周期温度冲击条件下焊点的疲劳状态演变实际上是由于焊点及其周边材料之间的热膨胀系数差异导致的. 如图 1 所示, 影响一个焊点性能的材料包括电容本体材料、电容焊端材料、钎料、焊盘和 PCB 基材. 当焊接完成后, 电容焊端、钎料和焊盘三者以焊接的方式连为一体, 并且三者同为金属材料彼此之间的热膨胀系数相差较小, 这里将其统一简化为钎料进行考虑. 这样焊点在温度循

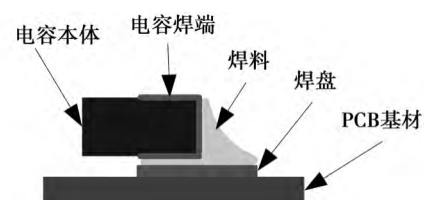


图 1 电容元件焊缝示意图

Fig. 1 Sketch map of capacitor welding line

收稿日期: 2015-01-08

基金项目: 吉林省科技发展计划资助项目(20126016)

环条件下的力学模型就演化为为了 PCB 基材、电容本体与钎料 3 种材料之间的问题。

焊锡爬升高度的计算。电容及焊盘尺寸示意图如图 2 所示。焊盘尺寸为 1.4 mm × 1.2 mm，钢网厚度为 0.2 mm，焊膏中钎料的体积约为 1/2，则单个焊盘的钎料体积为 0.168 mm³。元器件焊端与 PCB 焊盘的搭接面积约为焊盘面积的 1/2。计算最大爬锡高度，假设电容焊端底部没有钎料，焊点截面近似为三角形，则最大爬锡高度约为 0.4 mm。最小爬锡高度，即经过回流焊接后，没有焊锡爬升到焊端。这里电容的厚度为 0.8 mm，因此焊锡的爬升高度应介于 0 ~ 1/2 之间。结合对实际焊接情况的观察，确定焊锡的爬升高度应为电容厚度的 2/5 左右。

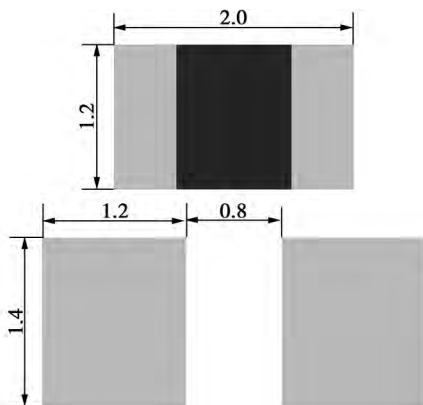


图 2 电容及焊盘尺寸图 (mm)

Fig. 2 Sketch map of capacitor and welding pad size

1.2 材料特性

试验用电容为 0805 封装，钎料、印制电路板基材以及电容元件本体材料特性如表 1 所示^[1]。

表 1 材料性能参数

Table 1 Material performance parameter

| 材料 | 热膨胀系数 $\alpha/10^{-6}K^{-1}$ | 弹性模量 E/GPa | 泊松比 μ |
|------------------|---------------------------------|-----------------------|--------------|
| Sn96.5/Ag3/Cu0.5 | 24.5 | 88 530 - 141.7T | 0.35 |
| FR4 | x 向 15; y 向 50 | 2.2×10^{-4} | 0.28 |
| EPOXY 树脂 | 13.8 | 1.42×10^{-4} | 0.3 |

1.3 温度循环载荷

约束条件模型变形的参考原点置于 PCB 板两端，即在 PCB 两端施加 x 和 y 向零位移约束。温度循环载荷：设定初始温度为 25 °C 时，焊点处于零应

力应变的初始状态。单个循环周期为 3 840 s，高温、低温保持时间各为 1 800 s，高温至低温、低温至高温转换时间各为 120 s。循环温度为 -40 ~ 100 °C，共 3 个周期。对于大多数金属材料，应力、应变出现周期性变化，循环 3 个周期后，塑性流动即可达到基本稳定状态^[1]。

1.4 结果分析

采用 UG9.0 软件进行试验仿真工作，在 Nx Nastran 模块下进行计算。元器件焊点的等效应变云图如图 3 所示。元器件焊点的等效应力云图如图 4 所示。从图 3 中可以看出，应变最大的位置发生在 PCB 基材、钎料与电容本体的交汇处。其本质是三种材料间的热膨胀系数不一致，在多周期温度冲击作用下，不同材料发生的形变量不一致，致使应力汇集。同时这里也是应变集中的区域。伴随着试验周期的增加，微裂纹开始在应力、应变集中区域率先萌生，并不断发展^[4-7]。监视、测量这一焊点疲劳发生、发展的过程，对于认识 Sn96.5/Ag3/Cu0.5 钎料在特定应用条件下的性能，发现其热疲劳性能劣化规律都具有重要的意义。

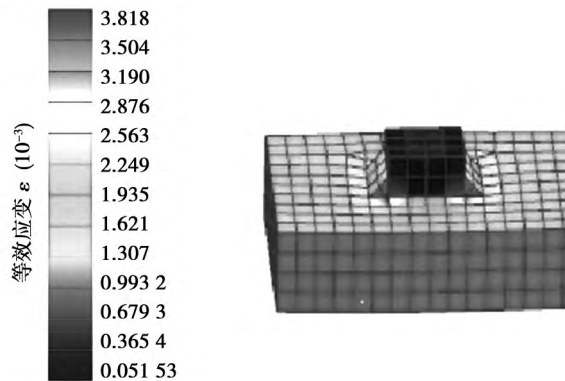


图 3 焊点等效应变分布

Fig. 3 Equivalent stress nephogram of soldering joint

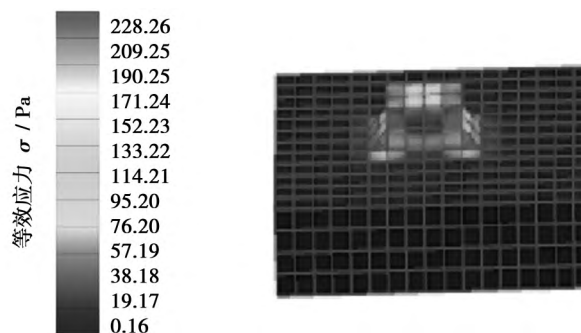


图 4 焊点等效应力分布

Fig. 4 Equivalent strain nephogram of soldering joint

2 焊点热疲劳寿命试验

温度循环作为自然环境的模拟, 可以考核产品在不同环境条件下的适应能力. 但无论如何, 试验条件下都不可能模拟出产品真实使用状态下的环境条件变化情况. 因此以应力循环周期数(通常为热应力或机械应力)来表征产品疲劳寿命的方法是存在一定局限性的. 但以应用较为成熟的有铅焊点为参照, 通过加速疲劳寿命的比较研究, 得到无铅焊点相对于有铅焊点的特性比较结论, 这对于认识无铅钎料的特性却有着重要的意义^[7, 8]. 针对焊点疲劳损伤的形成机制, 设计了焊点热疲劳状态测试的试验方法. 整个试验流程分为试验样本制备、温度冲击试验和剪切力测试3个部分.

2.1 试验样本

试验样本共焊接12块电容板, 采用Sn96.5/Ag3/Cu0.5钎料和Sn63/Pb37钎料各焊接6块. 焊接方法采用设备回流焊接, 图5为Sn96.5/Ag3/Cu0.5焊点的焊接曲线, 图6为Sn63/Pb37焊点的焊接曲线. 每块板中有10个0805封装的电容作为试验样本.

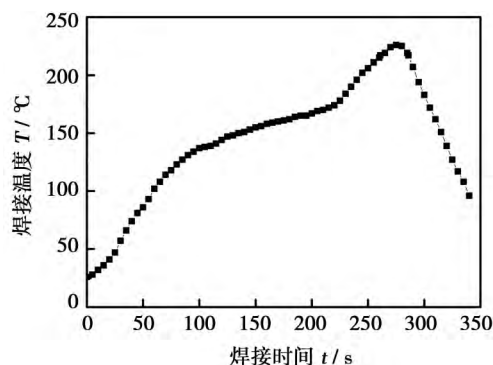


图5 Sn96.5/Ag3/Cu0.5 钎料回流焊接曲线

Fig. 5 Reflow soldering curve of Sn96.5/Ag3/Cu0.5

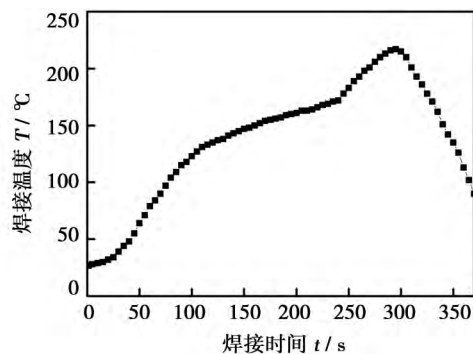


图6 Sn63/Pb37 钎料回流焊接曲线

Fig. 6 Reflow soldering curve of Sn63/Pb37

2.2 焊点温度冲击试验

温度循环条件为-40~100°C, 高温、低温保持时间均为30min, 温度转换时间为30s. 整个试验共进行1500个周期, 每300个周期为一个数据采样点, 取出一组印制电路板进行焊点剪切力测试, 从0~1500个周期共设置6个数据采样点.

2.3 焊点剪切力测试

焊点剪切力试验就是采集在各个疲劳状态下一定数量焊点的剪切力值, 并以剪切力值反映焊点所处的疲劳水平. 将各个疲劳状态的剪切力值, 用合适的曲线进行拟合, 就能够得到有限试验周期内焊点疲劳状态的变化曲线.

2.3.1 测试方法

试验根据日本标准JIS Z 3198-7《芯片产品的焊料切割检测方法》, 在WDW-500万能试验机上进行. 试验主要分为如下步骤. (1) PCB固定. 将PCB固定于专用工装之上并适当调整推刀与PCB之间的缝隙, 该缝隙应保持在0.2mm±0.05mm为宜. (2) 开机. 开启机器, 传感器校准, 建立待测样本文件夹并编号. (3) 测试并记录. 启动测试按钮, 推刀匀速推进直至将电容推离焊盘, 此时测试软件记录下整个剪切力值变化曲线, 自动提取曲线峰值. 重复步骤(3)直至测试完成全部试验样本.

2.3.2 测试结果

试验获得了Sn96.5/Ag3/Cu0.57焊点和Sn63/Pb37焊点各6组共120个剪切力值, 取每组10个样本的剪切力均值, 整理如表2所示.

表2 焊点剪切力试验数据

Table 2 Shearing test data of soldering joint

| 周期 T_1 (个) | Sn96.5/Ag3/Cu0.5 焊点剪切力均值 F/N | Sn63/Pb37 焊点 剪切力均值 F/N |
|-----------------|-----------------------------------|-----------------------------|
| 0 | 71.925 | 67.406 |
| 300 | 68.383 | 65.138 |
| 600 | 64.549 | 63.882 |
| 900 | 58.729 | 58.236 |
| 1 200 | 47.900 | 48.509 |
| 1 500 | 39.004 | 34.393 |

3 数据处理及分析

表2中的数据在坐标系中表现为一些离散的数据点, 通过观察可以发现这些数据点之间呈现出一种非线性关系. 采用曲线方程(1), 并通过非线性最小二乘法求取拟合参数^[8], 即

$$y = A - ae^{bx} \quad (1)$$

式中: A 为未经过温度冲击试验的焊点剪切力值; a ,

b 为方程系数; x 为周期数.

3.1 非线性最小二乘 Gauss-Newton 算法

采用非线性最小二乘 Gauss-Newton 算法, 通过 Matlab 编程, 运行程序后得到的参数 a , b 的拟合值和置信度均为 95% 的置信区间, 如表 3 所示. 由此可得电容元件 Sn63/Pb37 焊点的热疲劳状态拟合方程为 $y = 67.406 - 1.2765e^{0.6538x}$, Sn96.5/Ag3/Cu0.5 焊点的热疲劳状态拟合方程为 $y = 71.929 - 2.8949e^{0.4952x}$.

表 3 焊点热疲劳状态拟合参数

Table 3 List of solder joints' thermal fatigue state equation

| 焊点类别 | 参数 a | 参数 b | a 参数置信区间 | b 参数置信区间 |
|------------------|--------|--------|--------------------|--------------------|
| Sn96.5/Ag3/Cu0.5 | 2.8949 | 0.4952 | [0.5721 1.9809] | [0.5360 0.7716] |
| Sn63/Pb37 | 1.2765 | 0.6538 | [0.7722 5.0172] | [0.3330 0.6575] |

3.2 结果分析

对试验数据及焊点热疲劳拟合曲线进行分析如下. (1) 表 2 中的剪切力均值数据随循环周期的增加而逐渐减小, 这客观说明了焊点热疲劳现象的发生, 并且采用剪切力值能够表征焊点的热疲劳状态; (2) 根据表 2 中的数据, 截至 1 500 个周期, Sn96.5/Ag3/Cu0.5 焊点剪切力均值下降 45.77%, Sn63/Pb37 焊点剪切力均值下降 48.98%. 这说明在有限的 1 500 个周期内 0805 封装电容的 Sn96.5/Ag3/Cu0.5 焊点的热疲劳劣化速率略慢于 Sn63/Pb37 焊点; (3) 截止 1 500 个周期, Sn96.5/Ag3/Cu0.5 焊点的剪切力均值为 39.004 N 高于 Sn63/Pb37 焊点的 34.393 N. 这说明在 1 500 个有限周期内 Sn96.5/Ag3/Cu0.5 焊点的热疲劳性能优于 Sn63/Pb37 焊点.

4 结 论

(1) 在文中试验条件下, 0805 封装电容元件 Sn63/Pb37 焊点的热疲劳状态拟合方程为 $y = 67.406 - 1.2765e^{0.6538x}$, Sn96.5/Ag3/Cu0.5 焊点的热疲劳状态拟合方程为 $y = 71.929 - 2.8949e^{0.4952x}$.

(2) 在有限的 1 500 个周期内 0805 封装电容的 Sn96.5/Ag3/Cu0.5 焊点的热疲劳劣化速率略慢于 Sn63/Pb37 焊点.

(3) 在 1 500 个有限周期内 Sn96.5/Ag3/Cu0.5 焊点的热疲劳性能优于 Sn63/Pb37 焊点.

参考文献:

- [1] 周 斌, 邱宝军, 罗道军. 片式元件焊点的热循环应力应变模拟技术研究[J]. 电子元件与材料, 2008, 27(7): 58-61.
Zhou Bin, Qiu Baojun, Luo Daojun. Study on simulation technology of stress-strain for chip component soldering joint under thermal cycles [J]. Electronic Components and Materials, 2008, 27(7): 58-61.
- [2] 王 斌, 黄春跃, 李天明. 热循环加载片式元器件带空洞无铅焊点的可靠性[J]. 电子元件与材料, 2011, 30(6): 66-69.
Wang Bin, Huang Chunyue, Li Tianming. Reliability of chip components lead-free solder joints with voids under thermal cycle [J]. Electronic Components and Materials, 2011, 30(6): 66-69.
- [3] 魏鹤琳, 王奎升. 考虑 IMC 影响的 PBGA 无铅焊点温度循环有限元数值模拟[J]. 焊接学报, 2012, 33(1): 109-112.
Wei Helin, Wang Kuisheng. Numerical simulation of PBGA lead-free solder joints with consideration of IMC layer under thermal cycling condition [J]. Transactions of the China Welding Institution, 2012, 33(1): 109-112.
- [4] 吴玉秀, 薛松柏, 张 玲, 等. QFP 组件的优化模拟及焊点热疲劳寿命的预测[J]. 焊接学报, 2006, 27(8): 99-102.
Wu Yuxiu, Xue Songbai, Zhang Ling, et al. Optimum simulation and prediction on thermal fatigue life of soldered joints of QFP devices [J]. Transactions of the China Welding Institution, 2006, 27(8): 99-102.
- [5] Basaran C, Desai C S, Kundu T. Thermal mechanical finite element analysis of problems in electronic packaging using the disturbed state concept [J]. ASEM Journal of Electronic Packaging, 1998, 120(2): 41-53.
- [6] Lee S W, Zhang X. Sensitivity study on material properties for the fatigue prediction of solder joints under cyclic thermal loading [J]. Circuit World, 1998, 24(3): 26-31.
- [7] 胡永芳, 薛松柏, 禹胜林. QFP 结构微焊点强度的试验[J]. 焊接学报, 2005, 26(10): 78-80.
Hu Yongfang, Xue Songbai, Yu Shenglin. Study on strength of soldered microjoints of QFP decices [J]. Transactions of the China Welding Institution, 2005, 26(10): 78-80.
- [8] 刘 焱, 接 勤, 谢海峰, 等. 共振型气体泵用压电振子的疲劳寿命[J]. 光学精密工程, 2013, 21(4): 941-947.
Liu Yan, Jie Meng, Xie Haifeng, et al. Fatigue life of piezoelectric actuator used in resonance-type air pump [J]. Optics and Precision Engineering, 2013, 21(4): 941-947.

作者简介: 毛书勤, 男, 1982 年出生, 博士, 高级工程师. 主要从事电装工艺、可靠性研究工作. 发表论文 20 余篇. Email: maosq@ciomp.ac.cn

extra thin-plate joints.

Key words: extra thin plate; length of weld; inherent strain; welding deformation; finite element

Process stability evaluation on aluminum alloy twin-wire PMIG welding by approximate entropy based SVM of voltage signal ZHOU Xiaoxiao¹, WANG Kehong¹, YANG Jia-jia¹, HUANG Yong¹, ZHOU Zhilan² (1. School of Materials Science and Engineering, Nanjing University of Science and Technology, Nanjing 210094, China; 2. Department of Computer Science, The University of North Carolina at Chapel Hill, Chapel Hill 27514, USA) . pp 107 – 111

Abstract: An approximate entropy (ApEn)-support vector machine (SVM) method of arc voltage was proposed to evaluate the stability of aluminum alloy twin-wire pulse metal insert gas (PMIG) welding process. A set of welding experiments were carried out and the ApEn of welding current and voltage signals was calculated. The results showed that the smaller the ApEn of current and voltage signals is the more stable, the welding process is. The application of ApEn on the welding current and the welding voltage was compared. It showed that the voltage based ApEn is sounder in measuring the stability of aluminum alloy twin-wire PMIG welding. Then a support vector machine (SVM) algorithm based on approximate entropy (ApEn) has been developed on voltage signals. And the results of the classification showed that the SVM algorithm based on ApEn can mark off the stable processes from the unstable ones. When the training data is more than 20% , the classification accuracy is more than 90% .

Key words: aluminum alloy; twin wire weld; stability; approximate entropy; support vector machine

Stress analysis and structure optimization of copper cylinders in 3D packaging JIANG Wei, WANG Lifeng (Harbin University of Science And Technology, Harbin 150080, China) . pp 112 – 116

Abstract: This paper analysed the whole stress of the 3D packaging structure and the local copper cylinders stress in the process of chip heating. And the three-dimensional structure was optimized by using finite element simulation software ANSYS. The result showed that the maximum stress was distributed at the location between the outer corner and the bottom of the copper cylinder. The structural parameter was optimized taking the maximum stress of the copper cylinders as a response. The orthogonal optimization method including three factors and three levels was adopted, varied factors being copper cylinder diameter, the copper cylinder height and the copper cylinder pitch. The result showed that the copper cylinder diameter had the maximum effect on the stress, the copper cylinder height had the weakest influence, the effect of copper cylinder pitch was moderate. What's more, with the increase of the three factors mentioned above, the maximum equivalent stress between the outer corner and the bottom of the copper column decreased gradually.

Key words: finite element simulation; stress of copper column; orthogonal experiment; parameter optimization

Comparative studies on thermal fatigue performance to Sn96.5/Ag3/Cu0.5 solder joints of chip capacitor MAO Shuqin^{1,2}, LIU Jian¹, GE Bing¹ (1. Changchun Institute of Optics, Fine Mechanics and Physics, Chinese Academy of Sciences, Changchun 130031, China; 2. University of Chinese Academy of Sciences, Beijing 100039, China) . pp 117 – 120

Abstract: With the use of Pb in a variety of occasions prohibited, Lead-free technology becomes one of important research direction. For understanding the fatigue properties of

lead-free solder, there is important significance to analyse fanalyse state of lead-free solders and to research on the method of testing. With the 0805 chip capacitor device package solder joints as the research object, Sn96.5/Ag3/Cu0.5 solder joints finite element model is established for multi period under temperature cycles. And shearing test is carried out. The value of Period-shearing stress to Sn96.5/Ag3/Cu0.5 and Sn63/Pb37 solders is obtained. Thermal fatigue fitting curves of solder in 1 500 periods is acquired, by using nonlinear least square method to fit curves. The results indicates that under the stipulated test condition, in limited 1 500 periods, thermal fatigue performance of Sn96.5/Ag3/Cu0.5 solder joints' rate of thermal fatigue deterioration to 0805 capacitance is slightly slower than that of Sn63/Pb37 solder joints.

Key words: chip component soldering joint; thermal fatigue state; shearing force

Ultrasonic welding process of Cf/PPS with thermal radiant preheating and the fracture of welded joint XU Zhiwu¹, LI Zhengwei¹, LIU Jianguang², JIANG Wei¹, YAN Jiuchun¹ (1. State Key Laboratory of Advanced Welding and Joining, Harbin Institute of Technology, Harbin 150001, China; 2. Beijing Key Laboratory of Civil Aircraft Structure and Composite Materials, Beijing Aeronautical Science & Technology Research Institute of COMAC, Beijing 102211, China) . pp 121 – 124

Abstract: The feasibility of ultrasonic welding process on carbon fiber reinforced polyphenylene sulfide (Cf/PPS) composites with thermal radiant preheating was investigated. The effect of preheating temperature and welding pressure on the formation of bonding interface and the mechanical strength of welded joint was focused on. It was shown that increasing preheating temperature improved the fusion of the resin at the bonding interface and 100% of bonding area was achieved with a preheating temperature of 110 °C. The bonding area increased with the welding pressure and it reached 100% when the welding pressure exceeded 3 bars. The strength of the welded joint was enhanced with the welding pressure, but it declined at a welding pressure beyond 3 bars. The welded joint had a maximum strength of 20 MPa at a preheating temperature of 110 °C with a welding pressure of 3 bar.

Key words: ultrasonic welding; Cf/PPS composites; microstructure; preheating temperature

Microstructure and performance analysis of vacuum brazing welded titanium joints in honeycomb sandwich panel structure SHANG Lei¹, WANG Gang², YANG Dachun¹, LI Yao¹ (1. Center for Composite Material, Harbin Institute of Technology, Harbin 150001, China; 2. National Key Laboratory of Advanced Welding Production Technology, Harbin Institute of Technology, Harbin 150001, China) . pp 125 – 128

Abstract: The processing parameter of titanium alloy honeycomb sandwich structure was studied, using filling foil of Ti-Zr-Ni-Cu based metal. The vacuum degree was not lower than 2×10^{-3} Pa and the brazing temperature was 930 °C with a holding time of 30 min. The ultrasonic testing(NDT) results showed an excellent brazing weld with no welding-off and faulty welding. The microstructure of the brazed joint was examined by means of scanning electron microscopy(SEM) and energy dispersive spectroscopy (EDS) . The results showed that mutual diffusion was happened between the filler metal and the base metals resulting in the precipitation of new phases. Using the optimized parameters, the average tensile strength of joint was 12.8 MPa, the shear strength was 9.01 MPa. The fracture mode of the vacuum brazing joints belonged to a brittle type fracture

Key words: TC4 Honeycomb sandwich construction; brazing; microstructure; NDT; tensile strength